Available online at www.sciencedirect.com

ScienceDirect

PHOTONICS AND NANOSTRUCTURES Fundamentals and Applications

Photonics and Nanostructures – Fundamentals and Applications 12 (2014) 340–349

www.elsevier.com/locate/photonics

Bright and dark spatial solitons in metallic nanowire arrays

David E. Fernandes, Mário G. Silveirinha *

University of Coimbra, Department of Electrical Engineering, Instituto de Telecomunicações, 3030-290 Coimbra, Portugal

Received 5 February 2014; received in revised form 8 April 2014; accepted 17 April 2014
Available online 2 May 2014

Abstract

We investigate the formation and propagation of bright and dark three-dimensional unstaggered spatial solitons with cylindrical symmetry in a nonlinear nanowire metamaterial. The metamaterial is formed by metallic nanowires embedded in a Kerr-type dielectric host and is modeled using an effective medium approach. Unlike conventional Kerr media, the metamaterial supports bright solitons when the host is a self-defocusing material and dark solitons when the host is a self-focusing material. Our numerical calculations show that the confinement of the spatial-solitons results from the interplay of the host nonlinear response strength and the hyperbolic dispersion of the photonic states in the nanowire array. Subwavelength solitary beams may be observed for sufficiently strong nonlinearities.

Keywords: Metamaterials; Spatial solitons; Bright solitons; Dark solitons; Effective medium theory; Nanowire array

1. Introduction

In the recent years there has been a growing interest in reducing the characteristic size of photonic devices, as the race for small operating devices, compared to the operation wavelength, is always in demand. In this context, metallic nanowire arrays provide many opportunities for the manipulation of electromagnetic radiation on a subwavelength scale [1–4]. It was predicted that subwavelength stable spatial solitons can be formed in a metallic nanowire array embedded in a nonlinear Kerr-type dielectric [5–7]. Other families of plasmonic lattice solitons were investigated in Refs. [8,9]. The theoretical framework of these studies is based on coupled mode theory, which provides a somewhat limited physical understanding of the formation mechanism of the solitons in the metamaterial. More recently, Ref. [10] put forward an effective medium model for the nonlinear nanowire metamaterial. This approach regards the structure as a continuous medium characterized by a few effective parameters [10]. Based on such a theory, it was demonstrated in Ref. [7] that two-dimensional (2-D) unstaggered (i.e. modes that vary slowly in the scale of the period of the metamaterial) bright spatial solitons can only be formed if the host medium is a self-defocusing material. Here, we will show that this analysis can be further extended to characterize the propagation of three-dimensional (3-D) spatial solitons with cylindrical symmetry and dark solitons. Dark temporal and dark spatial solitons consist of dip-like shapes in the amplitude of a constant wave background [11–15]. The phase of spatial dark solitons has odd symmetry, and depending on

* Corresponding author. Tel.: +351 239 796268.
E-mail addresses: dfernandes@co.it.pt (D.E. Fernandes), mario.silveirinha@co.it.pt (M.G. Silveirinha).

http://dx.doi.org/10.1016/j.photonics.2014.04.003
1569-4410/

the dip amplitude in the constant wave background, they can be classified as either "black" dark spatial solitons, when the dip drops to zero and the phase is flat, or "gray" if the dip does not go to zero and the phase is not flat [12,13]. Bright and dark temporal solitons in metamaterial structures were reported in [16–18].

The organization of the article is as follows. In Section 2, we review the effective medium model of the nonlinear wire metamaterial and the conditions for the formation of solitary waves. In Section 3 we present numerical calculations for two distinct families of bright spatial solitons with cylindrical symmetry, highlighting the impact that structural parameters and losses have on wave propagation. A similar study is reported in Section 4, but for dark spatial solitons. In Section 5 the conclusions are drawn. This work assumes a time variation of the type $e^{-i\omega t}$, with ω the oscillation frequency.

2. Effective medium model and trapped states

The uniaxial wire medium is formed by a set of infinitely long parallel metallic wires, typically arranged in a square lattice with period a. The wires have radius r_w and complex permittivity ε_m. Here, we consider that the host medium is a nonlinear Kerr-type dielectric material such that the electric permittivity, for a fixed frequency, can be expressed as $\varepsilon = \varepsilon_h^0(1+\delta\varepsilon)$, where $\delta\varepsilon = \alpha \mathbf{e}^*\cdot\mathbf{e}$ is a nonlinear function of the microscopic electric field and $\alpha = 3\chi^{(3)}/\varepsilon_{h,r}^0$ is proportional to the third order electric susceptibility $\chi^{(3)}$ of the host medium. The metamaterial geometry is sketched in Fig. 1.

In the homogenization model developed in Ref. [10], the dynamics of the electromagnetic field is described

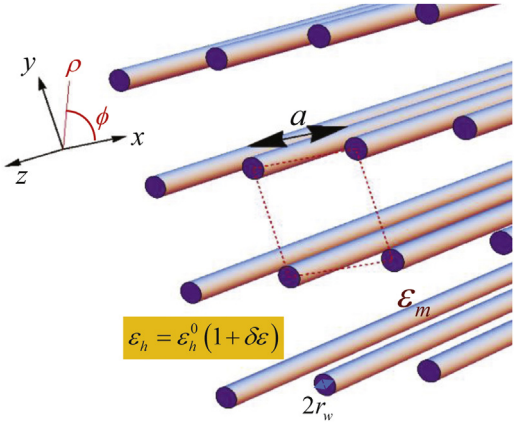

Fig. 1. Geometry of the periodic array of metallic nanowires embedded in a nonlinear Kerr-type host material.

by an eight component state vector $(\mathbf{E},\mathbf{H},\varphi_w,I)$ that satisfies a nonlinear first-order partial-differential system of equations. Here, $\mathbf{E}$ and $\mathbf{H}$ represent the macroscopic electromagnetic field (after spatial averaging of the microscopic fields $\mathbf{e}$ and $\mathbf{h}$), I is the current that flows along the nanowires (interpolated in a such a manner that it is defined over all the space) [19] and φ_w is a quasistatic potential defined as the average potential drop measured from the center of the wire to the boundary of the unit cell [19].

From Ref. [7,10] it is known that in the absence of external optical sources and for paraxial (quasi-transverse) optical beams propagating along the z-direction, $(\mathbf{E},\varphi_w)$ satisfy the following second-order nonlinear partial-differential system:

$$\nabla\times\nabla\times\mathbf{E} - k_h^2 n_{ef,h}^2\mathbf{E} = \frac{\beta_p^2}{\zeta_w}\left(\frac{\partial\varphi_w}{\partial z} - E_z\right)\hat{z}, \tag{1}$$

$$\frac{\partial^2\varphi_w}{\partial z^2} + k_h^2\zeta_w n_{ef,h}^2\varphi_w = \frac{\partial E_z}{\partial z}, \tag{2}$$

where $k_h^2 = \omega^2\varepsilon_h^0\mu_0$, $\zeta_w = 1-(Z_w/i\omega L)$, $Z_w = -(1/i\omega\pi r_w^2(\varepsilon_m-\varepsilon_h^0))$ is the per unit length (p.u.l.) self-impedance of the nanowires [19], $L = (\mu_0/2\pi)\log(a^2/4r_w(a-r_w))$ is the p.u.l. inductance of the wires [19] and $\beta_p = a^{-1}\sqrt{\mu_0/L}$ is the geometrical component of the plasma wave-number of the effective medium [19]. The parameter $n_{ef,h}^2$ is the effective (squared) normalized refractive index of the host medium defined by:

$$n_{ef,h}^2 \approx 1 + \alpha\mathbf{E}_t^*\cdot\mathbf{E}_t \tag{3}$$

where $\mathbf{E}_t = E_x\hat{\mathbf{x}} + E_y\hat{\mathbf{y}}$ is the transverse component of the electric field. Even though we are interested in paraxial beams, it is not possible to neglect E_z because in wire media the permittivity along the z direction can be extremely large, and thus the normalized z-component of the electric displacement D_z/ε_0 typically has a magnitude comparable to $\mathbf{E}_t$. It is useful to note that for waves such that the variation along z is of the form $e^{ik_z z}$, Eq. (1) can be written as

$$\nabla\times\nabla\times\mathbf{E} - \omega^2\mu_0\bar{\bar{\varepsilon}}_{eff}(\omega,k_z)\cdot\mathbf{E} = 0 \tag{4}$$

where we introduced a nonlocal dielectric function $\bar{\bar{\varepsilon}}_{eff}(\omega,k_z)$ that satisfies:

$$\frac{1}{\varepsilon_h^0}\bar{\bar{\varepsilon}}_{eff}(\omega,k_z) = n_{ef,h}^2\bar{\bar{I}} - \frac{1}{\zeta_w}\frac{\beta_p^2}{(k_h^2 - k_z^2/n_w^2)}\hat{\mathbf{z}}\hat{\mathbf{z}}. \tag{5}$$

The parameter $n_w^2 \approx \zeta_w n_{ef,h}^2$ is the slow-wave factor [10,19], such that an increase in n_w^2 reduces the effects of spatial dispersion. Note that $\bar{\bar{\varepsilon}}_{eff}(\omega,k_z)$ is a nonlinear

function of the transverse electric field because $n^2_{ef,h}$ also is. In this level of approximation, the nonlinear effects in the host medium are manifested in the macroscopic response simply by replacing the microscopic expression of the host permittivity $\varepsilon_h = \varepsilon_h^0(1 + \alpha \mathbf{e}^* \cdot \mathbf{e})$ by the macroscopic formula $\varepsilon_h = \varepsilon_h^0(1 + \alpha \mathbf{E}_t^* \cdot \mathbf{E}_t)$.

From here, it should be evident that the characteristic equation for the TM (Transverse Magnetic)-polarized photonic modes is (i.e. for waves with a uniform field amplitude and a spatial variation $e^{i\mathbf{k}\cdot\mathbf{r}}$, where $\mathbf{k} = \mathbf{k}_t + k_z\hat{\mathbf{z}}$ is the wave vector) [10]:

$$\frac{k_t^2}{\varepsilon_{zz}} + k_z^2 = n^2_{ef,h} k_h^2, \quad \text{with} \quad \varepsilon_{zz} \equiv 1 - \frac{\beta_p^2}{\zeta_w n^2_{ef,h} k_h^2 - k_z^2}. \tag{6}$$

The dispersion of the photonic states depends on $n^2_{ef,h}$ and thus on the intensity of the optical field. For a fixed transverse component $\mathbf{k}_t$ of the wave vector, the dispersion relation (6) can be reduced to a quadratic polynomial equation in k_z^2. Thus, there are two different propagating eigenmodes: a q-TEM (quasi-Transverse Electromagnetic) mode and a TM mode [19,20]. In our study we are only interested in the q-TEM mode, as it has no cutoff frequency and is the only mode that propagates below the plasma frequency of the effective medium (frequency wherein $\varepsilon_{zz}(\omega, k_z) = 0$). Using Eq. (6) it is possible to calculate the isofrequency contours of the q-TEM mode. As is well-known, these curves correspond to hyperbolic contours [20,21] that depend on the structural parameters of the metamaterial [10]. So, to a first approximation, the effective medium can be regarded as a hyperbolic medium. Hyperbolic metamaterials are of great interest due to their applications in the negative refraction of light [22], optimization of radiative heat transfer [23], enhancement of Casimir interaction [24], novel light sources based on the Cherenkov effect [25,26], amongst many others [27]. In our case, since $n^2_{ef,h}$ is a function of the electric field amplitude, the dispersion of the photonic states also depends on the strength of the nonlinear effects.

From a qualitative point of view, the isofrequency contours are of particular importance to understand the formation mechanism of the self-trapped states. As already discussed in Ref. [7], for a fixed frequency ω_0, a bright spatial-soliton associated with the generic z-propagation constant k_{z0} is only allowed when (i) for a sufficiently strong field amplitude the medium supports photonic states with $k_z = k_{z0}$, and (ii) for weak field amplitudes there are no photonic states with $k_z = k_{z0}$ available. For instance, in standard self-focusing Kerr-type dielectrics the dispersion of the photonic states is $k^2c^2 = \omega^2 n^2$, where c is the speed of light in a vacuum and n is the refractive index. For self-focusing materials n grows with the optical field amplitude and the isofrequency surfaces are spherical, such that the radius of the surfaces increases with the field strength [Fig. 2i)]. Therefore, provided $k_{z0} > n_0\omega/c$, being n_0 the refractive index for weak field amplitudes, it is possible to fulfill simultaneously the aforementioned conditions (i) and (ii), and thus to have spatial solitons. This is illustrated in Fig. 2i), where it is seen that the

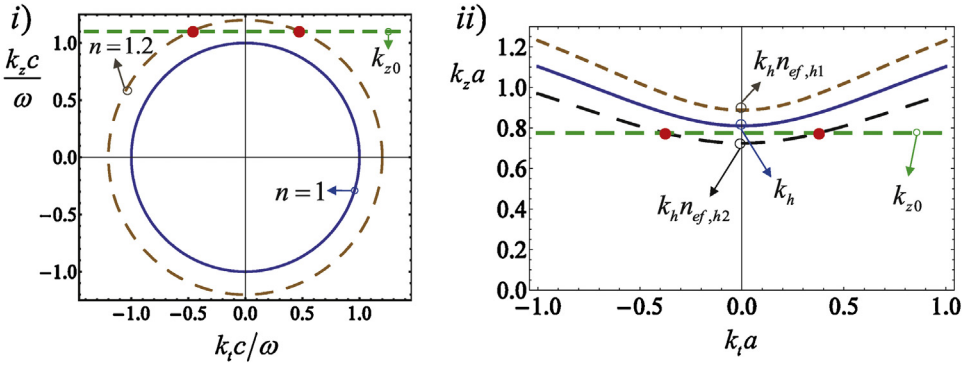

Fig. 2. Formation mechanism of the spatial solitons. Panel (i) Isofrequency contours of a conventional self-focusing Kerr dielectric for weak field amplitudes (solid blue line, $n = 1$) and for strong field amplitudes (long dashed brown line, $n = 1.2$). Panel (ii) Dispersion of the photonic states associated with the q-TEM mode in a silver nanowire material at $\lambda_0 = 1550$ nm. The nanowires are embedded in a dielectric background with $\varepsilon_h^0 = \varepsilon_0$, the lattice period is $a = 200$ nm, and the wire radius is $r_w = 0.1a$. The contours are calculated for: a self-focusing host material (dashed brown curves, $n^2_{ef,h1} = 1.2$), a self-defocusing host material (long dashed black curves, $n^2_{ef,h2} = 0.8$) and for a linear host (blue curves, $n^2_{ef,h} = 1.0$). The red dots correspond to a trapped state associated with $k_z = k_z0$ that is allowed only in case of sufficiently strong fields. For clarity, in the figures we consider large variations of n^2. (For interpretation of the references to color in this figure legend, the reader is referred to the web version of the article.)

green dashed horizontal line (photonic states with $k_z = k_{z0}$) only intersects the isofrequency contour associated with a strong field intensity (red dots in the picture).

A similar analysis can be done for the nanowire metamaterial. We start by reviewing the impact of the nonlinear response in the isofrequency contours of the effective medium. Using Eq. (6) we calculated the q-TEM modes dispersion for several values of $n^2_{ef,h}$ at $\lambda_0 = 1550$ nm. The metamaterial structural parameters are given in the caption of Fig. 2. It is supposed that the nanowires are made of silver. In the infrared domain, the complex permittivity ε_m of silver may be described by a Drude model, such that $\varepsilon_m - \varepsilon^0_h \sim \varepsilon_0(-\omega^2_m/\omega(\omega + i\Gamma))$ with a plasma frequency $\omega_m/2\pi = 2175$ THz and a collision frequency $\Gamma/2\pi = 4.35$ THz [31]. In Fig. 2ii the hyperbolic isofrequency contours of the photonic states are shown for the case of a weak field intensity (i.e. in the linear regime) [curve with $n^2_{ef,h} = 1.0$], and for the case of a strong field intensity. In the latter case, we consider two possibilities: (a) a self-focusing host medium, such that the third order electric susceptibility is positive, i.e. $\alpha > 0$ in Eq. (3) [curve with $n^2_{ef,h} > 1.0$], and (b) a self-defocusing host medium, such that $\alpha < 0$ [curve with $n^2_{ef,h} < 1.0$]. In these plots, the material loss was neglected. The change of topology of the isofrequency surfaces in this example as compared to Fig. 2i has notable consequences in the formation of bright spatial solitons. Indeed, it is geometrically evident that to fulfill the conditions (i) and (ii) enunciated earlier it is necessary that the line $k_z = k_{z0}$ is below the vertex of the hyperbola (point of the hyperbola where $k_t = 0$) associated with the linear regime (solid blue line). Therefore, under an effective medium framework, self-trapped states can only be formed when the dielectric host is a self-defocusing material [7]. Interestingly, even though the dielectric host medium is a self-defocusing material, the effective medium behaves as a self-focusing medium. However, it should be mentioned that it is possible to have staggered solitons when the host is a self-focusing material, but such solitary waves vary quickly on the scale of the unit cell of the metamaterial, and thus cannot be described using effective medium methods [6]. Examples of self-defocusing materials include the sodium vapor, some organic compounds, and some polymers [28–30].

The mechanism of formation of dark spatial solitons can also be understood with the help of the isofrequency contours. A dark spatial soliton may be seen as weakly guided mode with most of the field energy in the "cladding region", i.e. in the region with lowest refractive index. Thus, in conventional Kerr-type media, dark solitons are only allowed in case of a self-defocusing material [12–15]. For nanowire metamaterials the situation is exactly the opposite. Because the self-trapped state is weakly guided by "the core, now" one needs to impose that for low field intensities (core region) there are photonic states, while for strong field intensities (cladding region) photonic states are forbidden. The two conditions can be satisfied simultaneously only if the line $k_z = k_{z0}$ is above the vertex of the blue hyperbola in Fig. 2ii and below the vertex of the hyperbola associated with a strong field intensity. Evidently, this is only possible when the host is a self-focusing material. Thus, to have dark spatial solitons it is necessary that $k_h < k_{z0} < k_h n_{ef,h1}$ [see Fig. 2ii].

3. Bright spatial solitons

Next, we characterize two families of 3-D bright spatial solitons with cylindrical symmetry. Detailed parametric studies are presented to assess the confinement of the solitary waves and the impact of dielectric and metal absorption. It is supposed that the wires are made of silver and the losses in the dielectric are modeled by the loss tangent $\tan\delta$, such that $\varepsilon^0_h = \varepsilon_0(1 + i\tan\delta)$. Because we are interested in spatial solitons with cylindrical symmetry, it is convenient to use cylindrical coordinates, such that the transverse electric field is $\mathbf{E}_t = E_\rho\hat{\boldsymbol{\rho}} + E_\phi\hat{\boldsymbol{\phi}}$, where E_ρ, E_ϕ are the radial and azimuthal components of the electric field [Fig. 1].

3.1. Spatial solitons with cylindrical symmetry and $\mathbf{E}_t = E_\rho\hat{\boldsymbol{\rho}}$ and $\partial/\partial\phi = 0$

First, we consider a family of solitons such that the transverse electric field only has a radial component and a radial variation, i.e. $E_\phi = 0$ and $\partial/\partial\phi = 0$. In these conditions it can be checked that $\hat{\boldsymbol{\rho}} \cdot \nabla^2\mathbf{E} = \nabla^2 E_\rho - E_\rho/\rho^2$. Thus, calculating the inner product of both sides of Eq. (4) with $\hat{\boldsymbol{\rho}}$ we get:

$$\frac{\partial}{\partial\rho}\nabla\cdot\mathbf{E} - \nabla^2 E_\rho + \frac{E_\rho}{\rho^2} = k_h^2 n^2_{ef,h} E_\rho. \tag{7}$$

From Eq. (4) it follows that $\nabla\cdot[\bar{\bar{\varepsilon}}_{eff}(\omega, k_z)\cdot\mathbf{E}] = 0$ with $k_z = -i\partial_z$ ($\partial_u \equiv \partial/\partial u$). Neglecting the spatial variation of $n^2_{ef,h}$, this implies that $\nabla\cdot\mathbf{E} = \rho^{-1}\partial_\rho(\rho E_\rho)(1 - \varepsilon^{-1}_{zz})$ where $\varepsilon_{zz}(\omega, k_z)$ is defined as in Eq. (6). Substituting this result into Eq. (7), and writing $E_\rho = \tilde{E}_\rho(\rho, z)e^{ik_z z}$, where the envelope $\tilde{E}_\rho(\rho, z)$ is

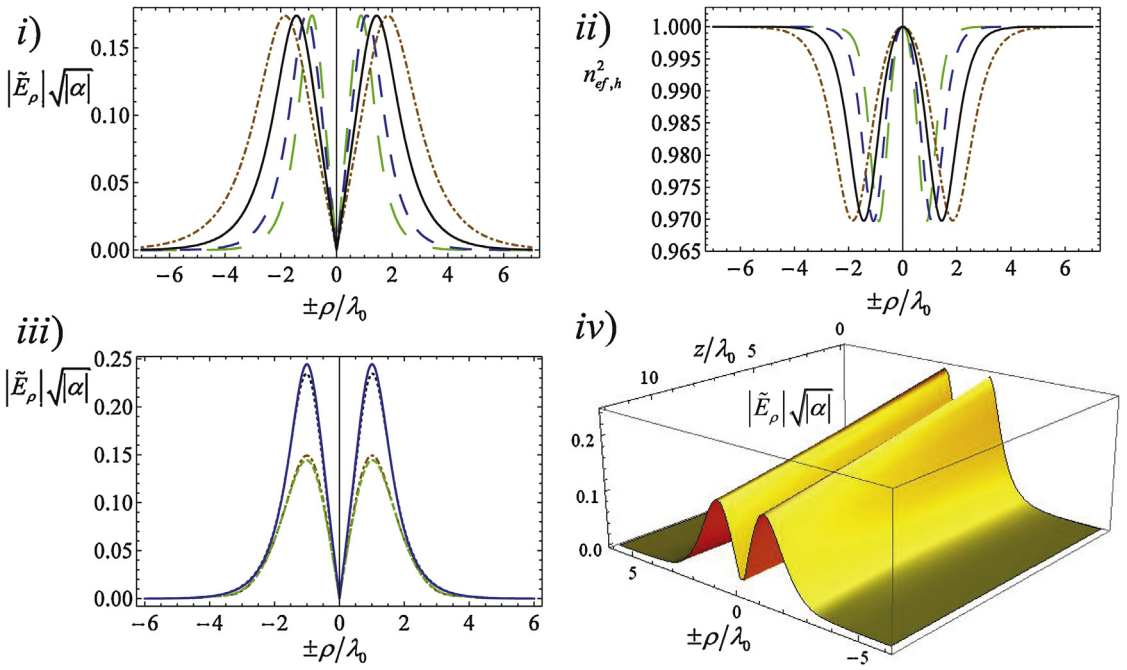

Fig. 3. Normalized field envelope $|\tilde{E}_\rho|\sqrt{|\alpha|}$ (panel i) and profile of the refractive index (panel ii) associated with a spatial soliton with $k_z = 0.995k_h$. The silver nanowire array is embedded in a dielectric host with $\varepsilon_h^0 = \varepsilon_0$, the nanowires radius is $r_w = 20$ nm and the lattice period and wavelength are such that: long dashed green lines: $r_w/a = 0.15$, $\lambda_0 = 1550$ nm; Solid black lines: $r_w/a = 0.1$, $\lambda_0 = 1550$ nm; Dashed-dotted brown lines: $r_w/a = 0.1$, $\lambda_0 = 1300$ nm; Dashed blue lines: $r_w/a = 0.15$, $\lambda_0 = 1300$ nm. Panel (iii) Normalized field envelope $|\tilde{E}_\rho|\sqrt{|\alpha|}$ for a spatial soliton with $k_z = 0.990k_h$ in a nanowire metamaterial with a dielectric host with $\varepsilon_h^0 = \varepsilon_0(1 + i\tan\delta)$ and silver nanowires with radius $r_w = 20$ nm, lattice period $a = 200$ nm, after a propagation distance of $12\lambda_0$ with $\lambda_0 = 1550$ nm. Solid blue curves: lossless case; Black dotted curves: with metallic loss; Dot-dashed brown curves: dielectric loss tangent $\tan\delta = 0.01$and no metallic loss; Green curves: with dielectric and metallic loss. Panel (iv) Profile of the spatial soliton as it propagates along the z-direction and both metal and dielectric absorption are considered. The structural parameters are as in panel (iii). (For interpretation of the references to color in this figure legend, the reader is referred to the web version of the article.)

supposed to vary slowly compared to the propagation factor, one finally finds that:

$$\frac{1}{\varepsilon_{zz}(\omega,k_z)}\left(\frac{\partial^2\tilde{E}_\rho}{\partial\rho^2}+\frac{1}{\rho}\frac{\partial\tilde{E}_\rho}{\partial\rho}-\frac{\tilde{E}_\rho}{\rho^2}\right)+2ik_z\frac{\partial}{\partial z}\tilde{E}_\rho = \left(k_z^2-k_h^2n_{ef,h}^2\right)\tilde{E}_\rho. \quad (8)$$

In the above, we used the approximation $\partial^2/\partial z^2 \to 2ik_z(\partial/\partial z) - k_z^2$, which follows from the hypothesis that the field envelope varies slowly. By solving the second order nonlinear differential Eq. (8) with suitable boundary conditions it is possible to compute the soliton profiles and their spatial evolution.

To determine the spatial solitons profile, we set the material loss parameters equal to zero and look for solution of Eq. (8) with $\partial_z = 0$, i.e. the field envelope is assumed independent of z. Because Eq. (8) is a second order differential equation, two initial conditions must be specified. Since $E_\phi = 0$ it is necessary that $\tilde{E}_\rho\big|_{\rho=0} = 0$. Thus, Eq. (8) is solved with $\partial_z = 0$ subject to:

$$\tilde{E}_\rho\big|_{\rho=0^+} = 0 \quad \text{and} \quad \left.\frac{\partial\tilde{E}_\rho}{\partial\rho}\right|_{\rho=0^+} = A, \quad (9)$$

where A is a constant that depends on k_z and on the structural parameters of the metamaterial. This constant is calculated iteratively by imposing that the field vanishes as $\rho \to +\infty$.

Fig. 3(i) shows the calculated soliton profiles for an array of silver nanowires embedded in a self-defocusing medium, for $k_z = 0.995k_h$ and different frequencies of operation and structural parameters. The electric field envelope is normalized to the strength of the nonlinear response (α). The numerical simulations confirm that bright solitons are allowed when the host medium is a self-defocusing material. Fig. 3ii shows the corresponding refractive index profiles. Consistent with the host type, it is seen that the refractive index is depleted in the regions of strong field intensity. Because the electric

field symmetry forces the radial component to be null at the origin, the electric field maximum is not centered at $\rho = 0$. Clearly, the structural parameters and the oscillation frequency have a significant influence on the characteristic beamwidth of the solitons [Fig. 3i)]. As already discussed in Ref. [7], typically the spatial confinement is determined by the degree of hyperbolicity of the isofrequency contours, such that for the same optical field intensity the confinement is poorer for metamaterials having more pronounced hyperbolic isofrequency contours. Highly hyperbolic isofrequency contours are obtained for dilute systems with small r_w/a (thin nanowires) and for short wavelengths of operation.

Moreover, in the limit wherein the metallic wires are perfectly electric conducting (PEC) ($\zeta_w = 1.0$, $n^2_{ef,h} = 1.0$) the isofrequency contours correspond to two flat parallel lines. Thus, in the PEC limit it is possible to have spatial-solitons with a vanishingly small nonlinear response [7]. Indeed, it is well known that for PEC nanowires the metamaterial supports diffractionless beams even in the linear regime [2,7,21].

To characterize the effect of loss, we solve again Eq. (8), now including the term $2ik_z\partial_z\tilde{E}_\rho$ and the parameters associated with dielectric and metal dissipation. The pertinent boundary conditions are such that $\tilde{E}_\rho(\rho, z = 0)$ is taken equal to the profile of the spatial soliton calculated in the absence of loss, and $\tilde{E}_\rho(\rho_{\max}, z) = 0$ where $\rho_{\max} >> W$ and W is the characteristic half-power beamwidth of the soliton [7]. In Fig. 3iii–iv we report the spatial evolution of a self-trapped wave with $k_z = 0.990k_h$ at $\lambda_0 = 1550$ nm for several lossy scenarios. Metal loss is modeled by setting the collision frequency parameter of the silver Drude model equal to $\Gamma/2\pi = 4.5$ THz [31], whereas dielectric loss is modeled by the loss tangent tan δ, as discussed previously. Consistent with Ref. [7], it is seen that the dominant absorption mechanism of the optical field is dielectric heating. Indeed, the effect of metallic loss may be negligible at $\lambda_0 = 1550$ nm, at least for the considered level of dielectric loss (tan $\delta = 0.01$). One of the reasons for this is that the light beam is a q-TEM beam, such that its energy is mostly concentrated in the dielectric region. Therefore, the optical field is much more sensitive to the absorption in the host medium rather than to the absorption in the metal.

3.2. Spatial solitons with cylindrical symmetry and $\mathbf{E}_t = E_\rho\hat{\boldsymbol{\rho}} + E_\phi\hat{\boldsymbol{\phi}}$

The soliton family studied in the previous subsection is such that the optical field vanishes at the beam center. This follows from the assumption that $E_\phi = 0$. Next, we investigate another soliton family where the optical field has a maximum at the beam center. Specifically, now we consider that $\mathbf{E}_t = E_\rho\hat{\boldsymbol{\rho}} + E_\phi\hat{\boldsymbol{\phi}}$ with $\partial_\phi = im$ and $m = \pm 1$.

To begin with, it is convenient to write the transverse part of the electric field as the gradient of a scalar potential ψ, such that,

$$\nabla_t\psi = E_\rho\hat{\boldsymbol{\rho}} + E_\phi\hat{\boldsymbol{\phi}} \tag{10}$$

where $\nabla_t = \partial_x\hat{\mathbf{x}} + \partial_y\hat{\mathbf{y}}$. Thus, in these conditions the electric field is given by $\mathbf{E} = \nabla_t\psi + E_z\hat{\mathbf{z}} = \nabla\psi + (E_z - \partial_z\psi)\hat{\mathbf{z}}$. Substituting this formula into Eq. (4), neglecting the spatial derivatives of $n^2_{ef,h}$, and using $\partial_z E_z = -(1/\varepsilon_{zz})\nabla_t^2\psi$ [which follows from $\nabla\cdot\left[\bar{\bar{\varepsilon}}_{eff}(\omega, k_z)\cdot\mathbf{E}\right] = 0$], it is possible to prove that Eq. (4) reduces to:

$$\nabla_t\left\{\frac{1}{\varepsilon_{zz}}\nabla_t^2\psi + \left(\frac{\partial^2}{\partial z^2} + k_h^2 n^2_{ef,h}\right)\psi\right\} = 0, \tag{11a}$$

$$\frac{1}{\varepsilon_{zz}}\nabla_t^2 E_z + \left(\frac{\partial^2}{\partial z^2} + k_h^2 n^2_{ef,h}\right)E_z = 0. \tag{11b}$$

In the above we put $\nabla_t^2 = \partial_x^2 + \partial_y^2$. Evidently, the obtained equations are nonlinear because from Eq. (3) we have $n^2_{ef,h} = 1 + \alpha|\nabla_t\psi|^2$. We are interested in optical beams with an angular variation of the form $e^{im\phi}$ where $m = \pm 1$ and ϕ is the azimuthal angle, such that the potential is written as $\psi = \tilde{\psi}(\rho)e^{ik_z z}e^{im\phi}$. Using again the approximation $\partial^2/\partial z^2 \to 2ik_z\partial_z - k_z^2$, it is found from Eq. (11a) that:

$$\frac{1}{\varepsilon_{zz}}\left(\frac{\partial^2}{\partial\rho^2} + \frac{1}{\rho}\frac{\partial}{\partial\rho} - \frac{m^2}{\rho^2}\right)\tilde{\psi} + \left(2ik_z\frac{\partial}{\partial z} - k_z^2 + k_h^2 n^2_{ef,h}\right)\tilde{\psi} = 0, \tag{12a}$$

$$n^2_{ef,h} = 1 + \alpha\left(\left|\partial_\rho\tilde{\psi}\right|^2 + \left|m\rho^{-1}\tilde{\psi}\right|^2\right). \tag{12b}$$

In order that the optical field is an analytic function of the spatial coordinates when $m = \pm 1$ all the even derivatives of $\tilde{\psi}$ with respect to ρ are required to vanish. Moreover, in order that the electric field is finite at the origin it is necessary that $E_\phi = imE_\rho$ at the origin or equivalently that:

$$\begin{aligned}&\tilde{\psi}\big|_{\rho=\rho_0=0^+} = A\rho_0 \quad \text{and}\\ &\left.\frac{\partial\tilde{\psi}}{\partial\rho}\right|_{\rho=\rho_0=0^+} = A, \quad (m = \pm 1).\end{aligned} \tag{13}$$

Thus, to find the spatial solitons Eq. (12) is solved with $\partial_z = 0$ subject to the above boundary conditions.

We also require that $\mathbf{E} \to 0$ in the limit $\rho \to +\infty$, which is tantamount to saying that $\partial_\rho \tilde{\psi} \to 0$ as $\rho \to +\infty$. For the bright soliton families studied in Ref. [7] and in the previous subsection, each value of $k_z < k_h$ corresponds a self-trapped wave, associated with a very specific value of the parameter A. We found out that for the family of solitons with $\partial_\phi = \pm i$ the situation is quite different. In fact, our numerical calculations show that all the bright solitons (i.e. the solutions of Eq. (12) with $\partial_\rho \tilde{\psi} \to 0$ as $\rho \to +\infty$) occur for $k_z = k_h$. Moreover, when $k_z = k_h$ any value of A yields a spatial soliton, such that as $|A| \to \infty$ the solitons become more and more confined. Notably, the point $k_z = k_h$ is coincident with the vertex of the isofrequency hyperbola in the linear regime (blue line in Fig. 2ii) [7]. It should be noted that the azimuthal variation of the optical field implies that $k_t \neq 0$, and hence there are no photonic states in the weak field regions when $k_z = k_h$. Thus the conditions (i) and (ii) enunciated in Section 2 are satisfied, as they should.

From a mathematical point of view it is also understandable that the solitons propagation constant is $k_z = k_h$. Indeed, taking the limit $\rho \to +\infty$ of both sides of Eq. (12a), and using $\partial_z = 0$, $n^2_{ef,h} \to 1$, $\partial_\rho \tilde{\psi} \to 0$ we find that $(-k_z^2 + k_h^2)\tilde{\psi} \to 0$. This is only possible if $k_z = k_h$ because $\tilde{\psi}$ does not have to approach zero in order that $\mathbf{E} \to 0$. Actually, our numerical simulations show that $\tilde{\psi}$ converges to a constant when $\rho \to +\infty$.

Fig. 4i depicts the calculated profile for a spatial soliton with $k_z = 1.0k_h$ at the wavelength $\lambda_0 = 1550$ nm. The silver nanowires have radius $r_w = 30$ nm and the lattice period is $a = 150$ nm. The absorption effects were discarded in the calculation. As expected, for this family of solitons the electric field does not vanish at the origin and the two components of the transverse electric field have the same amplitude at $\rho = 0$, such that the field is circularly polarized along the z-axis. As previously discussed, the auxiliary potential $\tilde{\psi}$ approaches a non-zero constant as $\rho \to +\infty$. Indeed to have $\mathbf{E} \to 0$ it is sufficient that $\partial_\rho \tilde{\psi} \to 0$ and $\tilde{\psi}/\rho \to 0$ for large radial distances. Because the envelope of the scalar potential tends to a fixed value, the radial electric field $\tilde{E}_\rho = \partial\tilde{\psi}/\partial\rho$ tends to zero faster than the azimuthal component which decays more slowly as $1/\rho$. Thus, the

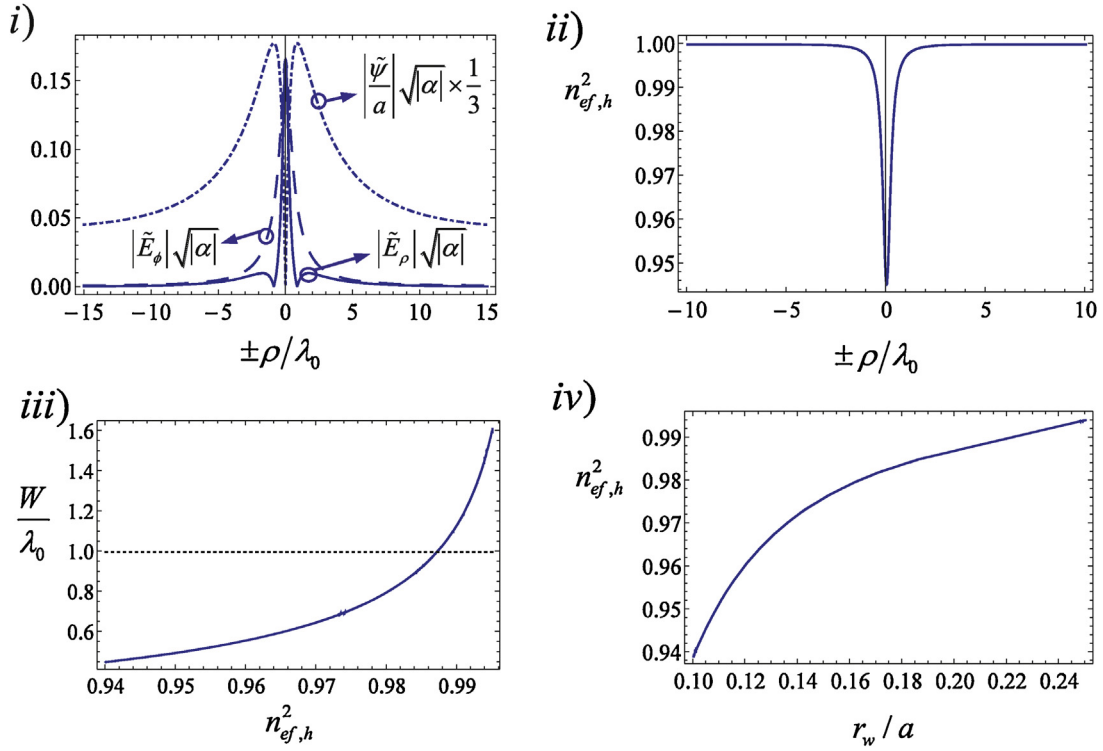

Fig. 4. Panel (i) Amplitude of the scalar potential $\left|\tilde{\psi}/a\right|\sqrt{|\alpha|}$ (dot-dashed curves) and normalized amplitude of the electric field envelope for the radial component $\left|\tilde{E}_\rho\right|\sqrt{|\alpha|}$ (solid lines) and azimuthal component $\left|\tilde{E}_\phi\right|\sqrt{|\alpha|}$ (dashed lines) as a function of the radial coordinate. Panel (ii) Profile of the refractive index. The spatial soliton has $k_z = 1.0k_h$ and propagates in a nanowire array embedded in a self-defocusing dielectric host with $\varepsilon_h^0 = \varepsilon_0$. The silver nanowires have radius $r_w = 30$ nm and the lattice period is $a = 150$ nm. Panel (iii) Normalized half-power beamwidth W as a function of $n^2_{ef,h}(\rho = 0)$. Panel (iv) Refractive index $n^2_{ef,h}(\rho = 0)$ required to have a subwavelength confinement ($W = 1.0\lambda_0$) as a function of r_w/a.

characteristic beamwidth of the azimuthal component of the electric field is significantly broader than that of the radial component.

Similar to the previous subsection, the confinement of the spatial solitons depends on the strength of the nonlinear effects. In Fig. 4iii we depict the half-power beamwidth of the spatial solitons as a function of the required value for $n^2_{ef,h}$ at $\rho = 0$. To have a subwavelength modal size ($W < \lambda_0$) it is necessary that $n^2_{ef,h} \approx 0.987$. In practice, such a large perturbation of the refractive index may be rather challenging to obtain. Fig. 4iv shows that the value of $n^2_{ef,h}$ that gives $W = \lambda_0$ depends significantly on the ratio r_w/a (in this plot the radius of the wires is varied and the remaining structural parameters are kept invariant). Consistent with the previous subsection, it is seen that nanowires with larger radius require weaker nonlinear effects for a comparable modal size. For instance for $r_w/a = 0.25$ subwavelength solitons can be achieved for $n^2_{ef,h} \approx 0.994$. The effects of metal and dielectric absorption are qualitatively analogous to what already reported in the previous subsection [not shown].

4. Dark spatial solitons

In this section we use the effective medium model to characterize 3-D dark spatial solitons with cylindrical symmetry. We are interested in dark spatial solitons with $E_\phi = 0$ and $\partial_\phi = 0$. The pertinent formalism is exactly as in Section 3-A, except that now we need to assume that the host material is a self-focusing Kerr dielectric with $\alpha > 0$. In particular, the dark spatial solitons satisfy Eq. (8). The boundary conditions (9) are also the same. However, now the parameter A is iteratively tuned so that the electric field tends to a non-zero constant value as $\rho \to +\infty$. Using the effective medium theory we calculated the dark solitons associated with $k_z = 1.005 k_h$ for different structural parameters and wavelengths of operation. The corresponding spatial soliton profiles are depicted Fig. 5.

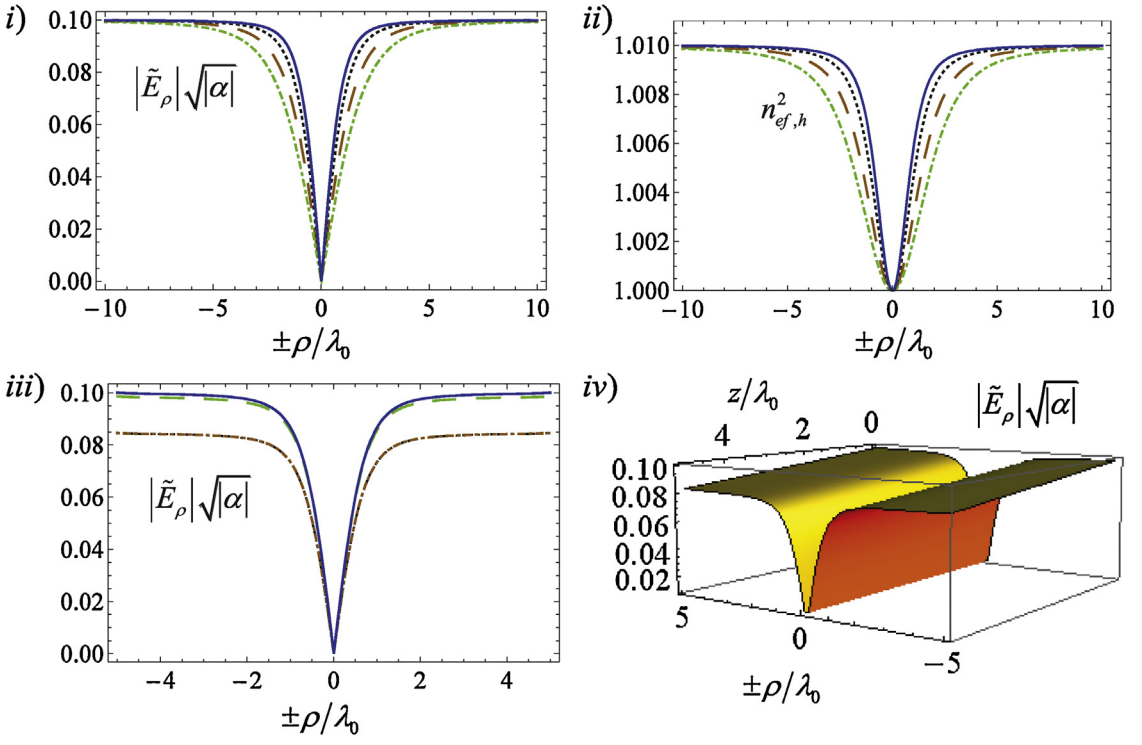

Fig. 5. Profile of (i) the radial electric field envelope $|\tilde{E}_\rho|\sqrt{\alpha}$ and (ii) refractive index associated with a spatial soliton with $k_z = 1.005 k_h$. The silver nanowire array is embedded in a self-focusing dielectric host with $\varepsilon_h^0 = \varepsilon_0$, has a lattice period $a = 200$ nm and the nanowire radius and the wavelength of operation are such that: Dot-dashed green lines: $r_w = 20$ nm, $\lambda_0 = 1300$ nm; Dotted black lines: $r_w = 30$ nm, $\lambda_0 = 1300$ nm; Solid blue lines: $r_w = 30$ nm, $\lambda_0 = 1550$ nm; Dashed brown lines: $r_w = 20$ nm, $\lambda_0 = 1550$ nm. Panel (iii) Normalized field envelope $|\tilde{E}_\rho|\sqrt{|\alpha|}$ for a dark spatial soliton with $k_z = 1.005 k_h$ in a nanowire metamaterial with a dielectric host with $\varepsilon_h^0 = \varepsilon_0(1 + i\tan\delta)$ and silver nanowires with radius $r_w = 30$ nm, lattice period $a = 150$ nm, after a propagation distance of $5\lambda_0$ with $\lambda_0 = 1550$ nm. Solid blue curves: lossless case; Green curves: with metallic loss; Dot-dashed brown curves: dielectric loss tangent $\tan\delta = 0.01$ and no metallic loss; Black dotted curves: with dielectric and metallic loss. Panel (iv) Profile of the spatial soliton as it propagates along the z-direction and both metal and dielectric absorption are considered. The structural parameters are as in panel (iii). (For interpretation of the references to color in this figure legend, the reader is referred to the web version of the article.)

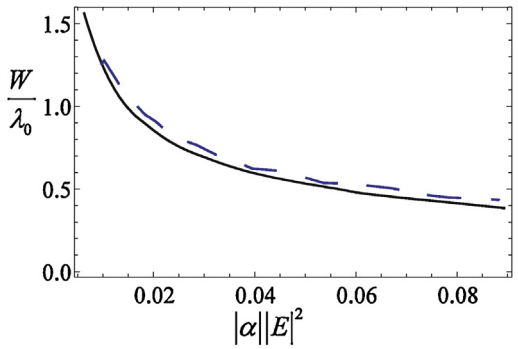

Fig. 6. Normalized half-power beamwidth W of 3-D spatial solitons as a function of the peak value of $|\alpha||E|^2$. The nanowire array is formed by lossless silver nanowires with radius $r_w = 30$ nm, lattice period $a = 150$ nm embedded in a dielectric host with $\varepsilon_h^0 = \varepsilon_0$ at the wavelength $\lambda_0 = 1550$ nm. Solid curve: bright solitons family; Dashed curve: dark solitons family.

As expected, the solitons consist of a dip-like shape in a constant wave background [12,13]. Moreover, because the electric field is null at the origin and the profile of the envelope phase is flat, these solitons are of the "black" type. Similar to Section 3-A, it is seen in Fig. 5i that the solitons characteristic size increases for thinner nanowires and shorter wavelengths of operation. The effect of dielectric and metal loss is illustrated in Fig. 5iii–iv, and is qualitatively analogous to what was found in Section 3 for the bright solitons. The strength of the nonlinear effects required to obtain a "black" dark soliton is also comparable to what is required by the bright solitons families previously studied. This is shown in Fig. 6 which depicts the half-power beamwidth of the spatial solitons as a function of the peak value of $|\alpha||E|^2$. The same figure also reports the beamwidth of the bright solitons family studied in Section 3-A. As seen, the beamwidth W is rather similar in the two cases.

5. Conclusions

Building on our previous studies [7,10], we investigated the formation and propagation of both dark and bright three dimensional spatial solitons in a nanowire array embedded in a Kerr-type nonlinear medium. It was demonstrated that within an effective medium framework, dark (bright) solitons can be formed only when the host medium is a self-focusing (defocusing) Kerr dielectric. We reported a numerical analysis that illustrates how the structural parameters of the metamaterial and the oscillation frequency affect the confinement of the solitary waves. It was confirmed that the main decay channel of the solitons is associated with dielectric absorption and that metal loss is typically of secondary importance. For a sufficiently large optical field intensity, the solitons can, in theory, become subwavelength. However, the required field strength may be rather difficult to achieve, especially for structures with thin nanowires ($r_w/a \ll 1$). The developed methods and ideas pave the way for further studies of nonlinear optics in nanowire structures.

Acknowledgements

This work was funded by Fundação para Ciência e a Tecnologia under project PTDC/EEI-TEL/2764/2012. D. E. Fernandes acknowledges support by Fundação para a Ciência e a Tecnologia, Programa Operacional Potencial Humano/POPH, and the cofinancing of Fundo Social Europeu under the fellowship SFRH/BD/70893/2010.

References

[1] C.R. Simovski, P.A. Belov, A.V. Atrashchenko, Y.S. Kivshar, Wire metamaterials: physics and applications, Adv. Mater. 24 (2012) 4229.
[2] P.A. Belov, Y. Hao, S. Sudhakaran, Subwavelength microwave imaging using an array of parallel conducting wires as a lens, Phys. Rev. B 73 (2006) 033108.
[3] P. Ikonen, C. Simovski, S. Tretyakov, P. Belov, Y. Hao, Magnification of subwavelength field distributions at microwave frequencies using a wire medium slab operating in the canalization regime, Appl. Phys. Lett. 91 (2007) 104102.
[4] G. Shvets, S. Trendafilov, J.B. Pendry, A. Sarychev, Guiding, focusing, and sensing on the subwavelength scale using metallic wire arrays, Phys. Rev. Lett. 99 (2007) 053903.
[5] Y. Liu, G. Bartal, D.A. Genov, X. Zhang, Subwavelength discrete solitons in nonlinear metamaterials, Phys. Rev. Lett. 99 (2007) 153901.
[6] F. Ye, D. Mihalache, B. Hu, N.C. Panoiu, Subwavelength plasmonic lattice solitons in arrays of metallic nanowires, Phys. Rev. Lett. 104 (2010) 106802.
[7] M.G. Silveirinha, Theory of spatial optical solitons in metallic nanowire materials, Phys. Rev. B 87 (2013) 235115.
[8] F. Ye, D. Mihalache, B. Hu, N.C. Panoiu, Subwavelength vortical plasmonic lattice solitons, Opt. Lett. 36 (2011) 1179.
[9] Y. Kou, F. Ye, X. Chen, Multipole plasmonic lattice solitons, Phys. Rev. A 84 (2011) 033855.
[10] M.G. Silveirinha, Effective medium response of metallic nanowire arrays with a kerr-type dielectric host, Phys. Rev. B 87 (2013) 165127.
[11] A. Hasegawa, F. Tappert, Transmission of stationary nonlinear optical pulses in dispersive dielectric fibers. II. Normal dispersion, Appl. Phys. Lett. 23 (1973) 171.
[12] Y.S. Kivshar, Dark solitons in nonlinear optics, IEEE J. Quantum Electron. 29 (1993) 250.
[13] Y.S. Kivshar, B. Luther-Davies, Dark optical solitons: physics and applications, Phys. Rep. 298 (1998) 81.

[14] S.A. Gredeskul, Y.S. Kivshar, Generation of dark solitons in optical fibers, Phys. Rev. Lett. 62 (1989) 977.
[15] S.A. Gredeskul, Y.S. Kivshar, Dark soliton generation in optical fibers, Opt. Lett. 14 (1989) 1281.
[16] G. D'Aguanno, N. Mattiucci, M. Scalora, M.J. Bloemer, Bright and dark gap solitons in a negative index Fabry-Pérot etalon, Phys. Rev. Lett. 93 (2004) 213902.
[17] M. Scalora, D. de Ceglia, G. D'Aguanno, N. Mattiucci, N. Akozbek, M. Centini, M.J. Bloemer, Gap solitons in a nonlinear quadratic negative-index cavity, Phys. Rev. E 75 (2007) 066606.
[18] G. D'Aguanno, N. Mattiucci, M.J. Bloemer, Ultraslow light pulses in a nonlinear metamaterial, J. Opt. Soc. Am. B 25 (2008) 1236.
[19] S.I. Maslovski, M.G. Silveirinha, Nonlocal permittivity from a quasistatic model for a class of wire media, Phys. Rev. B 80 (2009) 245101.
[20] M.G. Silveirinha, Nonlocal homogenization for a periodic array of ε-negative rods, Phys. Rev. E 73 (2006) 046612.
[21] M.G. Silveirinha, P.A. Belov, C.R. Simovski, Subwavelength imaging at infrared frequencies using an array of metallic rods, Phys. Rev. B 75 (2007) 035108.
[22] J. Yao, Z. Liu, Y. Wang, C. Sun, G. Bartal, A.M. Stacy, X. Zhang, Optical negative refraction in bulk metamaterials of nanowires, Science 321 (2008) 5891.
[23] C.R. Simovsky, S. Maslovski, I. Nefedov, A. Tretyakov, Optimization of radiative heat transfer in hyperbolic metamaterials for thermophotovoltaic applications, Opt. Express 21 (2013) 14988.
[24] T. Morgado, S. Maslovski, M. Silveirinha, Ultrahigh Casimir interaction torque in nanowire systems, Opt. Express 21 (2013) 14943.
[25] D.E. Fernandes, S.I. Maslovski, M.G. Silveirinha, Cherenkov emission in a nanowire material, Phys. Rev. B 85 (2012) 155107.
[26] V.V. Vorobev, A.V. Tyukhtin, Nondivergent Cherenkov radiation in a wire metamaterial, Phys. Rev. Lett. 108 (2012) 184801.
[27] C.L. Cortes, W. Newman, S. Molesky, Z. Jacob, Quantum nanophotonics using hyperbolic metamaterials, J. Opt. 14 (2012) 063001.
[28] G.A. Swartzlander Jr., D.R. Andersen, J.J. Regan, H. Yin, A.E. Kaplan, Spatial dark-soliton stripes and grids in self-defocusing materials, Phys. Rev. Lett. 66 (1991) 1583–1586.
[29] R.W. Boyd, G.L. Fischer, Nonlinear Optical Materials, Encyclopedia of Materials: Science and Technology, 2nd Ed., Elsevier, Oxford, 20016237–6244.
[30] L. Kamath, K.B. Manjunatha, S. Shettigar, G. Umesh, B. Narayana, S. Samshuddin, B.K. Sarojini, Investigation of third-order nonlinear and optical power limiting properties of terphenyl derivatives, Opt. Laser Technol. 56 (2014) 425–429.
[31] M.A. Ordal, R.J. Bell, R.W. Alexander Jr., L.L. Long, M.R. Querry, Optical properties of fourteen metals in the infrared and far infrared: Al, Co, Cu, Au, Fe, Pb, Mo, Ni, Pd, Pt, Ag, Ti, V, and W, Appl. Opt. 24 (1985) 4493.